First-principles insights on the magnetism of cubic SrTi1–xCoxO3–#

Citation: Florez, J. M., S. P. Ong, M. C. Onbas#li, G. F. Dionne, P. Vargas, G. Ceder, and C. A. Ross. "First-Principles Insights on the Magnetism of Cubic SrTi1–xCoxO3–δ." Appl. Phys. Lett. 100, no. 25 (2012): 252904. © 2012 American Institute of Physics.

As Published: http://dx.doi.org/10.1063/1.4729830

Publisher: American Institute of Physics

Persistent URL: http://hdl.handle.net/1721.1/91652

Version: Final published version: final published article, as it appeared in a journal, conference proceedings, or other formally published context

AIP | Applied Physics Letters

First-principles insights on the magnetism of cubic SrTi1−xCoxO3−δ

J. M. Florez, S. P. Ong, M. C. Onbaşli, G. F. Dionne, P. Vargas et al.

Citation: Appl. Phys. Lett. **100**, 252904 (2012); doi: 10.1063/1.4729830
View online: http://dx.doi.org/10.1063/1.4729830
View Table of Contents: http://apl.aip.org/resource/1/APPLAB/v100/i25
Published by the American Institute of Physics.

First-principles insights on the magnetism of cubic $SrTi_{1-x}Co_xO_{3-\delta}$

J. M. Florez,[1,2,a)] S. P. Ong,[1] M. C. Onbaşli,[1] G. F. Dionne,[1] P. Vargas,[2] G. Ceder,[1] and C. A. Ross[1,b)]
[1]*Materials Science and Engineering Department, MIT, Cambridge, Massachusetts 02139, USA*
[2]*Departamento de Física, Universidad Técnica Federico Santa María, Valparaíso, P.O. Box 110-V, Chile*

(Received 22 March 2012; accepted 30 May 2012; published online 19 June 2012)

We present hybrid density functional calculations suggesting that magnetism in cubic $SrTi_{1-x}Co_xO_{3-\delta}$ (STCO) with $x = 0.25$ is sensitive to the nearest neighbor arrangement of the Co and the presence of oxygen vacancies. Spin polarized calculations for $x = 0.25$ in which the nearest neighbor (nn) Co spacing is a, $\sqrt{2}a$ or $\sqrt{3}a$ with a the lattice parameter predict lowest energies for the $\sqrt{2}a$ nn separation and favor the ferromagnetic state. Oxygen deficiency ($\delta = 0.125$) lowers the average Co valence state and favors mixed valence and spin states (high spin for the Co adjacent to the vacancy and low for the non-adjacent Co), an increase of the band gap and an expansion of the lattice parameter compared to stoichiometric STCO in which both Co ions are low spin. Predicted configurations of the two neighboring Co ions are ($t_{2g}^5 e_g^0$, $t_{2g}^5 e_g^0$) and ($t_{2g}^4 e_g^2$, $t_{2g}^6 e_g^0$) with average 1.0 and 1.6 μ_B/Co for stoichiometric and 1-O-vacancy systems, respectively. © *2012 American Institute of Physics*. [http://dx.doi.org/10.1063/1.4729830]

Substituted $A_{1-y}A'_yB_{1-x}B'_xO_3$ perovskites are a rich source of potential technological applications due to the variety of ferroic order parameters that can be tuned via the specific cation or anion substituents[1–3] and because of their range of physical, chemical, and catalytic properties.[4,5] From both the multiferroic and the chemical viewpoint, oxygen stoichiometry plays a crucial role in defining the saturation magnetization, electric polarization, and chemical reactivity,[1–6] but the effects of oxygen stoichiometry on the electronic structure are still not completely understood. One interesting property is the room-temperature magnetism observed in magnetically substituted perovskites.[7,8] Most studies of magnetically substituted semiconductors have focussed on dilute levels of substitution, and there is still disagreement about the mechanisms driving spin ordering; in more highly magnetically substituted materials, there is also the possibility for exchange or other interactions between the magnetic ions, complicating the picture further. Magnetic ordering at room temperature has been observed experimentally in a range of highly substituted perovskites such as $SrTi_{1-x}M_xO_3$ (M = Fe, Co) where $x = 0.05$–0.5.[8–10] In these materials, the oxygen stoichiometry plays a major role in determining the magnetic properties because it affects the valence states of the magnetic ions and the lattice strain, which itself influences the magnetic properties via magnetoelastic effects.[8,9,11]

Non-magnetic $SrTiO_3$ (STO), which has a band gap of 3.25 eV, has been studied for its blue emission, superconductivity, giant thermopower, and ferroelectricity.[12–15] On the other hand, $SrCoO_3$ (SCO), which is a metallic ferromagnet, presents a useful sensitivity to magnetic and charge substituents and is a candidate for solid-state fuel cells.[16–19] The perovskite solid solution $SrTi_{1-x}Co_xO_3$ (STCO), can potentially integrate some of the properties of its end members, giving rise to interesting functionalities that may be useful in, for example, magneto-optical applications.[3,20,21] Recently, several substituted STCO-like systems have been studied,[5,8–10,18,22,23] but STCO itself has not been modeled and therefore its emergent properties remain unexplored, including the origin of its magnetic moment and order, the spin and valence states of the ions, and the importance of exchange coupling between magnetic ions, magnetoelastic effects, and the effect of oxygen vacancies. First-principles calculations can enable an understanding of intrinsic ordering and the effect of stoichiometry on the electronic and structural properties.[1,6,15,19]

In this letter, we study from first principles the dependence of total energy (TE) on the nearest-neighbor (nn) distance between Co ions, the Co valence states y and the oxygen deficiency δ in the $Sr^{+2}Ti^{+4}_{1-x}Co^{+y}_xO^{-2}_{3-\delta}$ system with $x = 0, 0.125, 0.25, 1$. Magnetic ordering, lattice parameters, and densities of states are determined for $\delta = 0.0, 0.125$ and several y valences. An increase of the optical band gap and a volumetric expansion are predicted as a response to non-zero δ, and the magnetization (μ_B/Co) depends on the presence of oxygen vacancies. We performed all calculations within density functional theory (DFT) as implemented in the Vienna Abinitio Simulation Package.[24] Because the purpose of the present investigation is to provide a model system to examine the influence of the valence and spin states of the Co ions on the TE, we used the recently implemented screened hybrid Heyd-Sceseria-Ernzerhof (HSE06) functional.[25–27] The HSE06 functional is a screened implementation of the Perdew-Burke-Ernzerhof (PBE) functional that combines the PBE exchange-correlation functional with the Hartree Fock (HF) exchange.[25–27] It has been shown to offer a substantial improvement upon semi-local DFT methods in several 3d oxides.[28,29] While the HSE06 functional does introduce two additional parameters (namely the HF mixing parameter a and the screening parameter ω), it avoids the U-J parametrization necessary in the LDA+U method. Spin-polarized calculations were performed using a plane-wave energy cutoff of 500 eV and the following k-point

a)E-mail: jmflorez@mit.edu.
b)E-mail: caross@mit.edu.

grids: $6\times6\times6$ for single unit cells of cubic STO and SCO (HSE06), $8\times8\times8$ for a comparison calculation of STO using GGA, and $2\times2\times2$ for the larger STCO unit cells (HSE06). Cubic perovskite supercells with 40 ($\delta=0.0$) and 39 atoms ($\delta=0.125$) were considered.

We first describe the STO and SCO structural and electronic features. The band gaps, relaxed lattice parameters, and local magnetic moments for S(T,C)O as calculated in this work are given in Table I. The experimental STO band gaps are 3.25 and 3.75 eV (Refs. 12–15) for direct and indirect transitions, respectively, but a comparative GGA calculation (not shown) underestimates the experimentally determined band gap by $\sim$1.4 eV. In an attempt to reproduce the experimental band gap, we used +U methods and concluded that physically unjustified Coulomb parameters are required to obtain a realistic band gap. The HSE06 calculation, however, predicts a band gap that is in fairly good agreement with experiments (Table I).

In the case of SCO, HSE06 predicts a metallic FM system, as observed for the cubic phase.[16,17] The lattice parameters in Table I are in good agreement with previous reports for STO and SCO.[12–19] Stoichiometric SCO could have low or high spin Co^{4+}, i.e., 1 or 5 μ_B, respectively. Experimentally, SCO (which grows with oxygen deficiency) shows a saturation magnetization of 2.1 or 2.5 $\mu_B/f.u.$,[16,17] leading to controversy concerning the valence and spin state of the Co. Intermediate spin configurations have been proposed for Co^{4+} attributed to partial transfer ($t_{2g}^{5-x}\rightarrow e_g^x$) or hybridization of high spin Co^{3+} ($t_{2g}^4\rightarrow e_g^2$) with oxygen partial holes antiferromagnetically coupled to neighboring Co-electrons of e_g symmetry.[17,30–32] These models, however, have not been compared with hybrid first-principles methods.

Table I presents four examples of SCO relaxation results from HSE06. In two cases, the Co ions were initialized with either $t_{2g}^5e_g^0$ (low) or $t_{2g}^3e_g^2$ (high) spin states S_i. Additionally, two calculations (indicated by *) were carried out with fixed magnetic moments per formula unit: one corresponding to the moment of Co^{4+}-low-spin ions, 1 μ_B, and one corresponding to the experimental result of 2.5 μ_B.[17] The calculations show that the $t_{2g}^3e_g^2$-initialized state relaxes to a much larger magnetic moment than that observed from experiments and has an unfavorable TE. On the other hand, the $t_{2g}^5e_g^0$-initialized state presents not just a lower energy than $t_{2g}^3e_g^2$ but it also self-consistently evolves to a higher moment of 1.8 $\mu_B/f.u.$. The lowest energy, marked "*gs*" (ground state), was obtained when the system was initialized with the experimental value of 2.5 $\mu_B/f.u.$, in which the resulting μ_B/Co reaches values close to $t_{2g}^4e_g^2$ occupancy, corresponding to an intermediate spin state.[16,17,30,31] Such saturation moments could also be tuned by using +U functionals, but there is no agreement on the appropriate U parameter for Co. For example, one calculation was based on a U chosen to yield 2.6 $\mu_B/f.u.$ corresponding to intermediate spin,[19] while another U value reported recently[33] was non-negligibly higher by $\sim$1.9 eV.[33] Before describing the STCO for $x=0.25$, we briefly analyze the case for $x=0.125$. In a $2\times2\times2$ STO supercell, we substitute one Ti with Co^{4+}. The calculation was done for low and high spin states (S_i) for both a fixed magnetic moment/*f.u.* (indicated by *) and an unconstrained magnetic moment. The results are presented in Table II. The lowest energy state *gs* is that in which the Co is in an intermediate spin state, with the next-lowest energy corresponding to the low spin state, as found for SCO. However, the energy difference between these states is between 10 and 20 times smaller for STCO than for SCO, when compared to the low spin state initialized SCO results (free and constrained).

We now describe the stoichiometric (i.e., no oxygen vacancy) $SrTi_{0.75}Co_{0.25}O_3$ system. A supercell consisting of 8 unit cells contains two Co ions, whose nn distance can be a, $\sqrt{2}a$ or $\sqrt{3}a$ (Fig. 1), where a is the cubic lattice parameter. By considering valence states that maintain a neutral supercell, i.e., Co^{4+}, and selecting the initial $\mu_B/f.u.$ to correspond

TABLE I. STO and SCO properties (E is given with respect to the ground state (*gs*) energy).

System	E_g (eV)	a'(Å)	a'/c'	μ_B/Ti, Co	$\mu_B/f.u.$	E (eV)
$SrTiO_3$	3.11	3.915	1.0001	0.0	0.0	—
$SrCoO_3$	0.0	3.840	0.9995	3.1	4.3	0.405
		3.831	1.0022	1.7	1.0*	0.229
		3.818	1.0073	2.1	1.8	0.109
		3.813	0.9952	2.6	2.5*	$\mathbf{0.0}_{gs}$

TABLE II. $Sr^{+2}Ti_{1-x}^{+4}Co_x^{+4}O_3^{-2}$ for one Co.

System	a'(Å)	S_i	μ_B/Co	$\mu_B/f.u.$	E (eV)(*per f.u*)
$SrTi_{1-x}Co_xO_3$	7.795	h	3.37	5.0	0.057
	7.795	h	3.35	5.0*	0.053
$x=0.125$	7.762	l	1.02	1.0*	0.012
	7.789	l	2.57	3.0	$\mathbf{0.0}_{gs}$

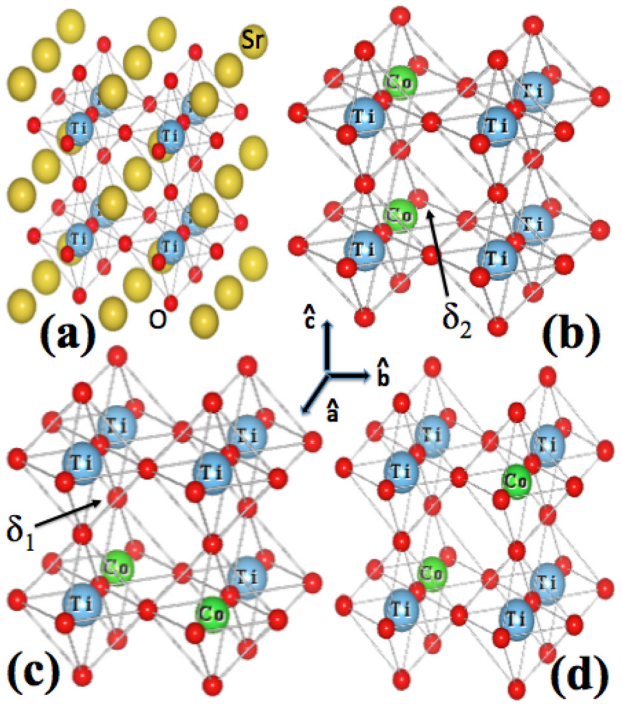

FIG. 1. $2\times2\times2$ supercells: (a) STO with lattice parameter a. (b–d) $SrTi_{0.75}Co_{0.25}O_3$ for Co nn distance (b) = a, (c) $\sqrt{2}a$, and (d) $\sqrt{3}a$. In (b–d), the Sr atoms are omitted.

TABLE III. $Sr^{+2}Ti^{+4}_{1-x}Co^{+4}_{x}O^{-2}_{3}$ properties for $x = 0.25$.

$E_{S_i}(perf.u.)$ for configurations in Fig. 1 with S_i Co spins				
nn_{Coi}	$E_{h_{AFM}}$(eV)	$E_{h_{FM}}$(eV)	$E_{l_{FM}}$(eV)	$E_{l_{AFM}}$(eV)
$a\sqrt{3}$	0.114	0.113	0.010	0.006
a	0.075	0.085	0.027	0.022
$a\sqrt{2}$	0.112	0.063	**0.000**$_{gs}$	**0.005**$_{us}$
Lattice parameters and magnetic structure				
State	$S_f^{1,2}$ (μ_B)	a'(Å)	a'/c'	V(Å^3)	E_g(eV)
us	$(1.0, 1.0)_{AFM}$	7.729	1.0011	460.45	1.60
gs	$(1.0, 1.0)_{FM}$	7.724	1.0012	460.27	1.61

to either low or high spin states, we performed calculations for both ferromagnetic and antiferromagnetic initial ordering, 12 cases in all. Table III compiles the computational results, in which we denote the initial Co nearest neighbor (nn) distance as nn_{Coi} and the energies as E_h for high spin initialization and E_l for low, with either FM or AFM ordering. Energies are given with respect to the lowest energy state, *gs*. For *gs* and *us*, which is the next highest energy state, the final Co spins are given as $S_f(\mu_B)$ and the relaxed lattice parameters as a' and c'. The final cubic structures are slightly distorted, and both *gs* and the unstable state *us* correspond to low-spin Co.

Table III predicts that the energy E_l is lower when the Co ions are separated by $\sqrt{2}a'$ or $\sqrt{3}a'$ instead of by a'. The $\sqrt{2}a'$ distance is most favorable and avoids sharing of any oxygen octahedral neighbors. Modeling predicts that the *gs* is a FM coupled configuration, containing $t_{2g}^5 e_g^0$ Co-spins with $1.0\,\mu_B/Co$. The similar occupancies giving rise to this value are nicely observed in Fig. 3(a). The energy band gap for *gs* and *us* is ~50% of the STO band gap. The results suggest that the tilting or rotation of the O-octahedra[1] caused by Co substitution compete with the interaction energy; in the $\sqrt{2}a'$ arrangement of the Co, the resulting pseudo-cubic nn_{Co} spacing is slightly larger than the initial spacing nn_{Coi}.

We then performed calculations in supercells with $nn_{Co} = \sqrt{2}a'$ and with $\delta = 0.125$ corresponding to one oxygen vacancy; henceforth the notation $(S^1, S^2) = S^{1,2}$ will be used, where S^1 identifies the Co ion at an incompletely O-coordinated B site and S^2 identifies the Co with complete

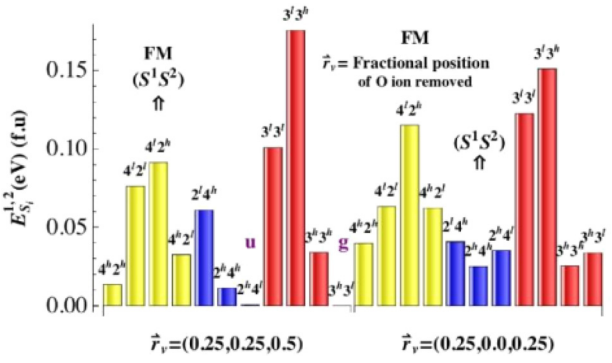

FIG. 2. FM energies for different valence spin states and O vacancies created at $\delta_{1,2}$. δ_1 provides *gs* and *us*.

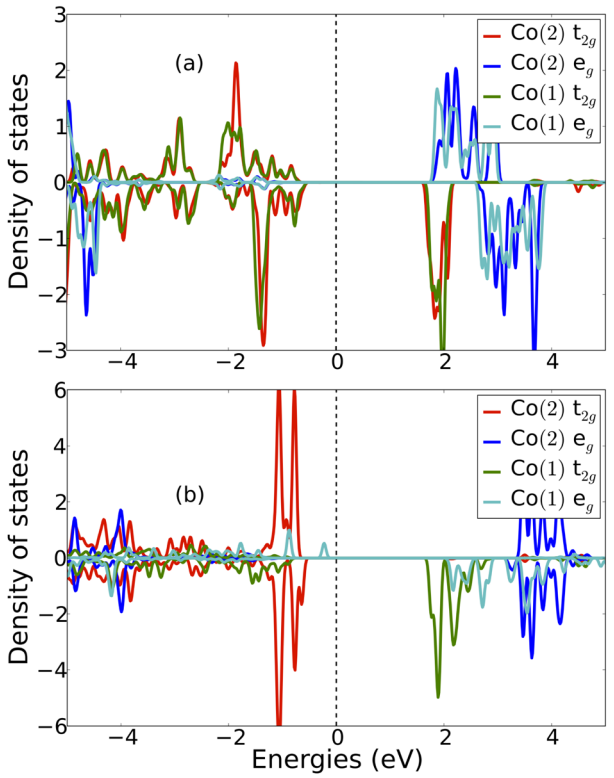

FIG. 3. Resolved t_{2g} and e_g density of states for Co ions: (a) Stoichiometric STCO (*g* state in Table III). (b) Oxygen deficient STCO (*g* state in Table IV).

O-coordination. Four different positions of the vacancy are possible, two of which were adjacent to the Co, labelled δ_1 and δ_2, which were expected to provide lower energies than the non-Co-adjacent vacancies. Fig. 1 shows δ_1, which lies at (0.25, 0.25, 0.5) in the (001) plane, along $\hat{c}$ with respect to the Co S^1 ion; δ_2 is at (0.25, 0, 0.25). The Co ions can both have $y = 3+$ valence states, or one can be 2+ and one 4+, and the spins can be high or low, and initially parallel (FM) or antiparallel (AFM). All 22 distinct possibilities were modeled for both vacancies, with δ_1 producing lower energy states (ground state). These are given in Table IV for the different Co valence and spin states including details of the lattice parameters and band gaps for the lowest energy state *gs* and the next lowest energy state, *us*. (The $S^{1,2} = 2, 4$ low, low case is equivalent to the $S^{1,2} = 4, 2$ low, low case.) In Fig. 2, we also present a comparison between the FM energies for δ_1 and δ_2. A complete study of all the possible vacancies would require consideration of changes in the Ti valence, which is beyond the scope of this work.

The model predicts Co^{3+} with mixed spin states as the *gs* in what seems to be $t_{2g}^4 e_g^2$ for S^1 and $t_{2g}^6 e_g^0$ for S^2, i.e., a well defined Co^{3+} (high, low) spin state, in contrast to the Co^{4+} (low, low) stoichiometric case shown as the *gs* in Table III. Such occupancies describing the magnetic moments in Table IV can be analyzed from the resolved density of states in Fig. 3(b). These stabilized magnetic moments present FM ordering, but since the completely oxygen-coordinated Co ion has almost no magnetic moment, this leads to an average $1.6\,\mu_B/Co$. This moment derives from just the Co (S^1) adjacent to the oxygen vacancy, and the other completely oxygen-coordinated Co (S^2) is sufficiently far away that no exchange interaction is expected. This is consistent with the

TABLE IV. $Sr^{+2}Ti^{+4}_{0.75}Co^{+y}_{0.25}O^{-2}_{3-\delta}$ properties for $\delta = 0.125$.

$E_{S_i^{1,2}}(per\ f.u.)$ for $nn_{Co} = a'\sqrt{2}$ with $S_i^{1,2}$ Co spins			
Valence	$S_i^{1,2}$	E_{AFM}(eV)	E_{FM}(eV)
$y_{1,2}$ =(4,2)	(*h*,*h*)	0.134	0.014
	(*l*,*l*)	0.097	0.076
	(*l*,*h*)	0.081	0.091
	(*h*,*l*)	0.008	0.033
$y_{1,2}$ =(2,4)	(*l*,*h*)	0.103	0.061
	(*h*,*h*)	0.075	0.011
	(*h*,*l*)	0.048	**0.001**$_{us}$
$y_{1,2}$ =(3,3)	(*l*,*l*)	0.112	0.101
	(*l*,*h*)	0.035	0.175
	(*h*,*h*)	0.027	0.034
	(*h*,*l*)	0.003	**0.000**$_{gs}$

Lattice parameters and magnetic structure					
State	$S_f^{1,2}(\mu_B)$	a'(Å)	a'/c'	V(Å^3)	E_g(eV)
us	$(3.1, 0.3)_{FM}$	7.7655	0.9987	467.99	1.73
gs	$(3.1, 0.1)_{FM}$	7.7568	0.9978	467.68	1.85

molecular orbital model, because Co^{3+}-low-spin ions cannot magnetically interact with Co^{3+}-high-spin ions because of their diamagnetic t_{2g}^6 state.[21,34] Therefore, the system can be described as consisting of two non-interacting sub-lattices: one made of magnetic Co^{3+}-high-spin ions and the other of diamagnetic Co^{3+}-low-spin ions.

The *us* in Table IV represents high spin Co^{2+} adjacent to the vacancy and coupled FM to low spin Co^{4+} in the other position. It displays an energy close to that of *gs*, and has almost the same net magnetic moment as *gs*. The half-filled e_g orbital in the Co^{2+} $t_{2g}^5 e_g^2$ and the empty e_g orbital in the Co^{4+} $t_{2g}^5 e_g^0$ would suggest a FM exchange-type interaction.[21,34] However, because the Co ions are not sharing an oxygen, no cation-anion-cation ABO_3 linkage rules[21,34] could intuitively anticipate the superexchange coupling. Taking into account, a complex exchange mechanism such as double exchange would be the only way to explain the FM, but on the basis of direct mechanisms and due to $nn_{Co} = \sqrt{2}a'$ exchange-type coupling would likely be weak. Nevertheless, the self-consistent calculations provided here show that *us* is in fact a FM state.

The oxygen-deficient STCO can therefore be described as a FM system without dominant exchange mechanisms. This is corroborated by the lowest energy AFM-initialized configuration, which turns out to be the AFM-initialized version of *gs*, i.e., the *gs* is not significantly sensitive to the local spin inversion because of either the diamagnetic Co or the weak orbital overlap. Such weak overlaps are perhaps better understood when we compare the FM-AFM energy difference for the *gs* for $\delta = 0$ and 0.125. Weakening of the exchange-type mechanisms is driven by the movement of the incompletely coordinated Co into the space left by the O-vacancy, which decreases the probability of superexchange coupling mediated by overlaps.

Comparing Tables II and III, we observe that creating an oxygen vacancy in STCO results in an increase in the volume of the unit cell, consistent with what is observed experimentally.[8–10] Second, the spin states of the magnetic ions at the incompletely coordinated B-sites increase when δ is non-zero. The third observation is that the direction along which the larger change in lattice parameter occurs is the direction joining the oxygen vacancy and Co. Finally, the optical band gap increases when the oxygen deficiency is introduced. The increase of the band gap is dominated by the change in the oxygen p orbitals near the Fermi level. The missing O^{2-} electrons lead to a half-filled p occupancy at the edge of the valence band.

Experimentally, films grown in oxygen have little magnetic moment while films grown in vacuum, which are oxygen deficient, contain mixed valence Co (or Fe in the case of Fe-substituted STO), a strong anisotropy attributed to magnetoelasticity, and moments of 0.5 to 1 μ_B/Co.[8–10] The films had a larger lattice parameter than STO due to the lower valence state and thus larger radii of the Co ions. The saturation magnetization did not follow a Brillouin function, indicating that exchange was not the dominant mechanism. These results are broadly consistent with the electronic structure determined from the hybrid calculations.

These results predict several electronic properties that could be explored in other ABO_3 systems, giving a further insight into the origin of the room temperature ferromagnetism of cubic perovskites. Calculated optical properties in Table IV are also of common interest as they show the dependence of the band gap on the oxygen deficiency. The band gap could determine the utility of such materials as multiferroic insulators, where wide gaps are preferred to preserve ferroelectricity,[1,7,13] or as photoactive generators, where narrow band gaps are required so that photoactivity is not restricted to the ultraviolet.[1,6,15] Given the integrability of perovskites on Si,[8–10] examination of their electronic properties using hybrid first-principles methods could provide guidance in materials selection for a wide range of devices based on these materials.

The authors acknowledge the National Science Foundation, and J.M.F. thanks Fondecyt postdoctorate 3110077 and DGIP-UTFSM (Chile) for financial support.

[1]J. M. Rondinelli and N. A. Spaldin, Adv. Mater. **23**, 3363 (2011).
[2]P. Zubko, S. Gariglio, M. Gabay, P. Ghosez, and J.-M. Triscone, Ann. Rev. Condens. Mater. Phys. **2**, 141 (2011).
[3]L. Bi, A. R. Taussig, H.-S. Kim, L. Wang, G. F. Dionne, D. Bono, K. Persson, G. Ceder, and C. A. Ross, Phys. Rev. B **78**, 104106 (2008).
[4]J. Suntivich, K. J. May, H. A. Gasteiger, J. B. Goodenough, S.-H. Yang, Science **334**, 9 (2011).
[5]D. J. Cumming, V. V. Kharton, A. A. Yaremchenko, A. V. Kovalevsky, and J. A. Kilnerz, J. Am. Ceram. Soc. **94**(9), 2993 (2011).
[6]K. M. Rabe, Annu. Rev. Condens. Matter Phys. **1**, 211 (2010).
[7]J. P. Velev, S. S. Jaswal, and E. Y. Tsymbal, Philos. Trans. R. Soc. A **369**, 3069 (2011).
[8]D. H. Kim, L. Bi, P. Jiang, G. F. Dionne, and C. A. Ross, Phys. Rev. B **84**, 014416 (2011).
[9]L. Bi, H.-S. Kim, G. F. Dionne, and C. A. Ross, New J. Phys. **12**, 043044 (2010).
[10]P. Jiang, L. Bi, D. H. Kim, G. F. Dionne, and C. A. Ross, Appl. Phys. Lett. **98**, 231909 (2011).
[11]G. F. Dionne, J. Appl. Phys. **101**, 09C509 (2007).
[12]D. S. Kan, T. Terashima, R. Kanda, A. Masuno, K. Tanaka, S. C. Chu, H. Kan, A. Ishizumi, Y. Kanemitsu, Y. Shimakawa, and M. Takano, Nature Mater. **4**, 816 (2005).

[13]M. Itoh, R. Wang, Y. Inaguma, T. Yamaguchi, Y. J. Shan, and T. Nakamura, Phys. Rev. Lett. **82**, 3540 (1999).
[14]A. Tkach, T. M. Correia, A. Almeida, J. Agostinho Moreira, M. R. Chaves, O. Okhay, P. M. Vilarinho, I. Gregora, and J. Petzelt, Acta Mater. **59**, 5388 (2011).
[15]T. Mizoguchi, N. Takahashi, and H.-S. Lee, Appl. Phys. Lett. **98**, 091909 (2011).
[16]P. Bezdicka, A. Wattiaux, J. C. Grenier, M. Pouchard, and P. Hagenmuller, Z. Anorg. Allog. Chem. **619**, 7 (1993).
[17]Y. Long, Y. Kaneko, S. Ishiwata, Y. Taguchi, and Y. Tokura, J. Phys.: Condens. Matter **23**, 245601 (2011).
[18]A. Baszczuk, B. Dabrowski, S. Kolesnik, O. Chmaissem, and M. Avdeev, J. Solid State Chem. **186**, 240 (2012).
[19]J. H. Lee and K. M. Rabe, Phys. Rev. Lett. **107**, 067601 (2011).
[20]L. Bi, J. Hu, P. Jiang, D. H. Kim, G. F. Dionne, L. C. Kimerling, and C. A. Ross, Nature Photon. **5**, 12 (2011).
[21]G. F. Dionne, *Magnetic Oxides* (Springer, New York, 2009).
[22]C. Pascanuta, N. Dragoeb, and P. Bertheta, J. Magn. Magn. Mater. **305**, 6 (2006).
[23]R. Garg, A. Senyshyn, H. Boysen, and R. Ranjan, Phys. Rev. B **79**, 144122 (2009).
[24]G. Kresse and J. Furthmller, *Vienna Ab Initio Simulation Package, Users Guide* (The University of Vienna, Vienna, 2009)
[25]J. Heyd, G. E. Scuseria, and M. Ernzerhof, J. Chem. Phys. **118**, 8207 (2003)
[26]J. Paier, M. Marsman, K. Hummer, G. Kresse, I. C. Gerber, and J. G. Angyan, J. Chem. Phys. **125**, 249901 (2006).
[27]J. Heyd, G. E. Scuseria, and M. Ernzerhof, J. Chem. Phys. **124**, 219906 (2006).
[28]V. L. Chevrier, S. P. Ong, R. Armiento, M. K. Y. Chan, and G. Ceder, Phys. Rev. B **82**, 075122 (2010).
[29]F. El-Mellouhi, E. N. Brothers, M. J. Lucero, and G. E. Scuseria, Phys. Rev. B **84**, 115122 (2011).
[30]R. H. Potze, G. A. Sawatzky, and M. Abbate, Phys. Rev. B **51**, 11501 (1995).
[31]M. Zhuang, W. Zhang, A. Hu, and N. Ming, Phys. Rev. B **57**, 13655 (1998).
[32]A. Van der Ven, M. K. Aydinol, G. Ceder, G. Kresse, and J. Hafner, Phys. Rev. B **58**, 2975 (1998).
[33]A. Jain, G. Hautier, S. P. Ong, C. J. Moore, C. C. Fischer, K. A. Persson, and G. Ceder, Phys. Rev. B **84**, 045115 (2011).
[34]J. B. Goodenough, J. Phys. Chem. Solids **6**, 287 (1958).